DOI: 10.1021/ma901570h

Macromolecules
ARTICLE

Toward the Photoinduced Reactivity of 1,5-Diphenylpenta-1,4-diyn-3-one (DPD): Real-Time Investigations by Magnetic Resonance

Arnulf Rosspeintner,[†] Markus Griesser,[†] Niklas Pucher,[‡] Kurt Iskra,[§] Robert Liska,[‡] and Georg Gescheidt*,[†]

[†]*Institute of Physical and Theoretical Chemistry, Graz University of Technology, Technikerstrasse 4/I, A-8010 Graz, Austria,* [‡]*Institute of Applied Synthetic Chemistry, Vienna University of Technology, Getreidemarkt 9/163, A-1060 Wien, Austria, and* [§]*Institute of Experimental Physics, Graz University of Technology, Petersgasse 16, A-8010 Graz, Austria*

Received July 17, 2009; Revised Manuscript Received September 10, 2009

ABSTRACT: The reactivity of 1,5-diphenylpenta-1,4-diyn-3-one (DPD) upon photolysis in acetonitrile and propan-2-ol was followed by continuous-wave time-resolved EPR (TR-EPR) and ^{1}H CIDNP (chemically induced dynamic nuclear polarization) spectroscopy. It was found that radical polymerizations using DPD can only be accomplished if an efficient hydrogen donor, such as propan-2-ol, is present, reflecting an analogous reaction pathway as the related benzophenone (BP). The same behavior was also established for ODPD, the bis(*p*-methoxy) derivative of DPD. In contrast to parent BP, where the steric hindrance of the ortho phenyl protons causes a twisted geometry, DPD and ODPD adopt an essentially planar minimum geometry which is also conserved in the corresponding radicals of type C as revealed by density functional theory calculations. This planarity is possibly one important factor for the considerable efficiency of DPD and its derivatives to act as initiators for two-photon-induced radical polymerizations.

1. Introduction

1,5-Diphenylpenta-1,4-diyn-3-one (DPD) is a novel photoinitiator for radical polymerization comprising the benzophenone (BP) chromophore, which is extended by symmetrically attached ethynyl moieties.[1] This extension leads to the desired and expected red-shifted electronic absorption band with respect to BP (by almost 1 eV). Surprisingly, DPD is also active under two-photon absorption conditions.[2]

The introduction of electron-donating substituents, such as methoxy groups (ODPD), into the *para* position of the phenyl moieties gives rise to bathochromic shifts of the optical absorption spectra.[3] However, the altered electronic structure by this donor substituent may also change the photoreactivity of parent DPD.[3,4]

Initial product analyses of irradiated reaction mixtures containing DPD and acrylates in propan-2-ol (IP) led to the assumption that the initiating step involves the formation of the propan-2-ol-2-yl radical (IP$^\bullet$) and radical C1$^\bullet$ derived from DPD via triplet-state H atom transfer (Scheme 1).[5]

Additionally, it was suggested that the initiation step with a monomer (e.g., butyl acrylate, BAC) is not based on radical C1$^\bullet$ but requires IP$^\bullet$.

The aim of this investigation is to establish the mechanism of the above reactions by detecting the primary species in real time using magnetic resonance spectroscopy. In particular, we apply time-resolved electron paramagnetic resonance (TR-EPR), which is a versatile technique for investigating transient radical species. It has already been successfully applied to, e.g., hydrogen abstraction reactions of benzophenone[6,7] and acetophenone,[8] the photochemistry of acetone and acrylate monomers in propan-2-ol,[9] or the α-cleavage of α-hydroxy ketones.[4] Moreover, we have used ^{1}H CIDNP (chemically induced dynamic nuclear polarization)[10−12] to reveal the primary products of the photoinduced reactions involving radicals. Density functional theory calculations (DFT) allow insight into the electronic properties of the reactive intermediates.

2. Experimental Section

1,5-Diphenylpenta-1,4-diyn-3-one (DPD) and 1,5-bis(4-methoxyphenyl)penta-1,4-diyn-3-one (ODPD) were synthesized and purified as described in ref 2. Benzophenone (BP) (Fluka, ≥99.0%), butyl acrylate (BAC) (Fluka, ≥99.0%), acetonitrile (ROTH, ≥99.9%), and propan-2-ol (IP) (ROTH, ≥99.9%) were used as received.

Continuous-wave time-resolved electron paramagnetic resonance (CW TR-EPR) experiments were performed using the pulses (355 nm, ca. 10 mJ/pulse, ca. 10 ns) from a frequency-tripled Continuum Surelite II Nd:YAG laser (20 Hz repetition rate), a Bruker ESP 300E X-band spectrometer (unmodulated static magnetic field), and a LeCroy 9400 dual 125 MHz digital oscilloscope. In the course of a TR-EPR experiment the desired magnetic field range is scanned by recording the accumulated (usually 50−100 accumulations) EPR time responses to the incident laser pulses at a given static magnetic field. The system is controlled using a software developed, kindly provided and maintained by Dr. J. T. Toerring.[13] Argon-saturated solutions were pumped (irreversibly, to avoid sample decomposition) through a quartz tube (inner diameter 2 mm, flow ca. 2−3 mL/min) in the reactangular cavity of the EPR spectrometer. The solutions were 0.5−10 mM in photoinitiator concentration, corresponding to absorbances of 0.3−3 at 355 nm for the quartz tubes used, while the butyl acrylate concentration was fixed to 0.1 M.

^{1}H NMR and CIDNP spectra were recorded on a 200 MHz Bruker AVANCE DPX spectrometer. Irradiation was carried out using a frequency-tripled Spectra Physics Nd:YAG laser (355 nm, ca. 40 mJ/pulse, ca. 10 ns) and a Hamamatsu (Japan) Hg−Xe lamp (L8252, 150 W, 300 ms). The following pulse sequence was used: presaturation−laser/lamp flash−30° RF

*Corresponding author. E-mail: g.gescheidt-demner@TUGraz.at.

 Published on Web 09/24/2009

detection pulse (2.25 μs)−free induction decay. The concentrations of the initiators were about 0.01 mM, and the excess of BAC/IP was about 1:5-fold.

The hyperfine coupling constants (hfc) of the BP and DPD ketyl radicals were calculated using the Gaussian03 package.[14] All calculations (geometry optimizations and single point calculations) were conducted at the B3LYP[15,16] level of theory with the basis set TZVP.[17]

3. Results and Discussion

3.1. General. The present investigation involved three sets of experiments: (i) The initial reaction of the photoinitiators (BP, DPD, and ODPD) in acetonitrile and propan-2-ol was investigated with CW TR-EPR spectroscopy to gain insight into the primary initiation mechanism. (ii) The experiments were repeated in the presence of butyl acrylate, serving as monomer, to identify the radical polymerization initiating species. (iii) Analogous photolyses were followed by the CIDNP technique.

3.2. TR-EPR: Reaction without/with Propan-2-ol. On the basis of the observation of photoproducts formed after excessive irradiation (up to 2 h), the reaction mechanism depicted in Scheme 1 was suggested.[5] Excitation of DPD or its derivatives leads to fast intersystem crossing from the excited singlet to the triplet state.

To inspect whether hydrogen abstraction is exclusively decisive for the performance of DPD, we have carried out the reaction in acetonitrile (a very weak hydrogen donor)[18] inside the TR-EPR spectrometer. Conspicuously, no signals were detected pointing to non-radical-pair involving reaction pathways are taking place. However, in the presence of propan-2-ol, the triplet state of DPD can undergo hydrogen abstraction, leading to the formation of radical pairs. This gives rise to the detection of photoinitiator-based radical C1$^\bullet$ and the propan-2-ol-2-yl radical (IP$^\bullet$). The latter radical is anticipated as the principal species inducing further polymerization.

In Figure 1, the CW TR-EPR spectra obtained after laser flash excitation of the argon-saturated propan-2-ol solutions of DPD are displayed. The central signal of the spectrum is split into two components (see also Figure 5). One of them represents the central component of the septet of radical IP$^\bullet$ (^{1}H hfc(CH_3) = 1.97 mT (6 equiv of H), g = 2.0026, the lines of the CW TR-EPR signal do not resemble the usual EPR intensity distribution because of radical-pair effects);[19] the other is characteristic for C1$^\bullet$ and can be further resolved (see Figure 4c). The CW TR-EPR spectra obtained upon irradiation of ODPD essentially reveal an identical pattern resembling that obtained from BP under comparable conditions.[7]

It is noteworthy that the hyperfine pattern of the signals assigned to C1$^\bullet$ (and C2$^\bullet$) points to a significant delocalization of the spin into the aromatic substituents via the triple bond, which is supported by DFT calculations of radicals C1$^\bullet$ and the analogous diphenylhydroxymethyl radical (B$^\bullet$) derived from benzophenone (BP). Table 1 compares the experimental and calculated isotropic hyperfine coupling constants (hfcs). The ^{1}H hfcs of the O*H* hydrogen atom and the *ortho* and *para* protons are rather similar, while those assigned to the *meta* protons are substantially smaller with a positive sign as indicated by theory. This shows that the unpaired electron in C1$^\bullet$ and B$^\bullet$ is delocalized within the entire π system. Whereas for B$^\bullet$ a planar geometry is not feasible owing to the steric hindrance by the *ortho* phenyl

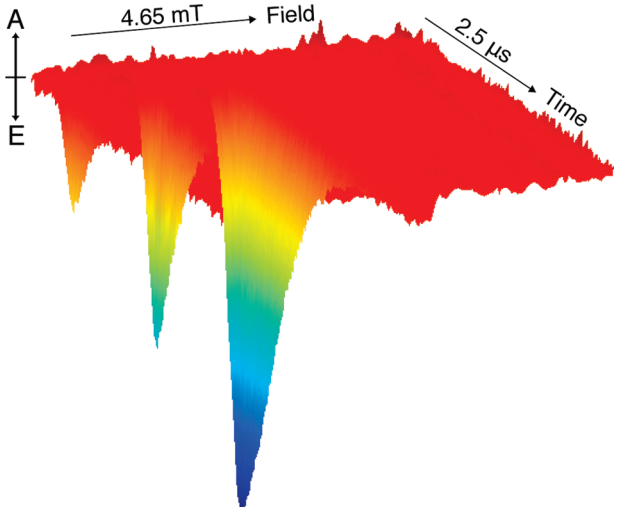

Figure 1. Time dependence of the CW TR-EPR spectrum of DPD in propan-2-ol, with A denoting absorption and E emission.

Table 1. Experimental and Calculated Hyperfine Coupling Constants (in mT) for Radicals C1$^\bullet$ and B$^\bullet$

	O*H*	H_o (4 equiv of H)	H_m (4 equiv of H)	H_p (2 equiv of H)
C1$^\bullet$ (exp)[a]	0.20	0.13	0.08	0.17
C1$^\bullet$ (calc)	−0.26[b]	−0.21	0.09	−0.23
B$^\bullet$ (exp)[20]	0.291	0.321	0.124	0.364
B$^\bullet$ (calc)	0.08[b]	−0.35	0.16	−0.39

[a] Owing to the substantial deviations of the intensity pattern of the experimental EPR spectrum (due to RPM and TM, see text), the simulation was accomplished by using the experimentally detected line distances and associating these with the calculated values; therefore, the error margin of the values given above is large (ca. 30%). [b] The calculated hfc for the OH proton refers to a (minimum-energy) orientation of the hydroxy group in which the H atom resides in the plane of the O atom and the (three) adjacent C atoms separated by one and two bonds. The barrier for rotation around the C−O bond is rather low and leads to substantially higher calculated hfc values for the OH proton (see Supporting Information).

Chart 1. Structures of the Investigated Photoinitiators

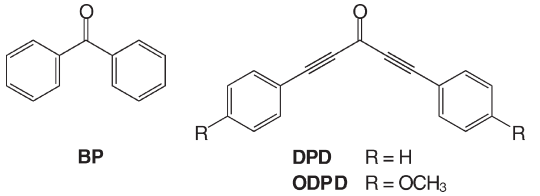

Scheme 1. Photoinduced Reactivity of DPD and ODPD in the Presence of IP

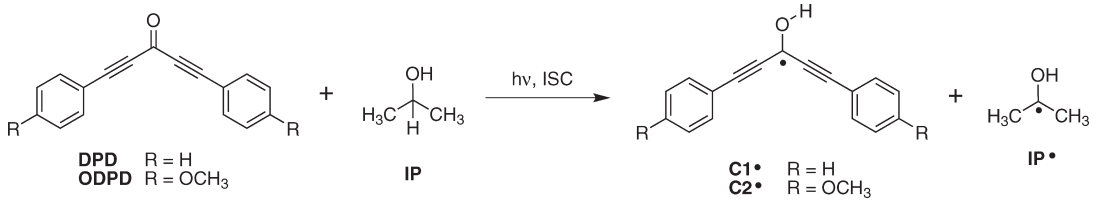

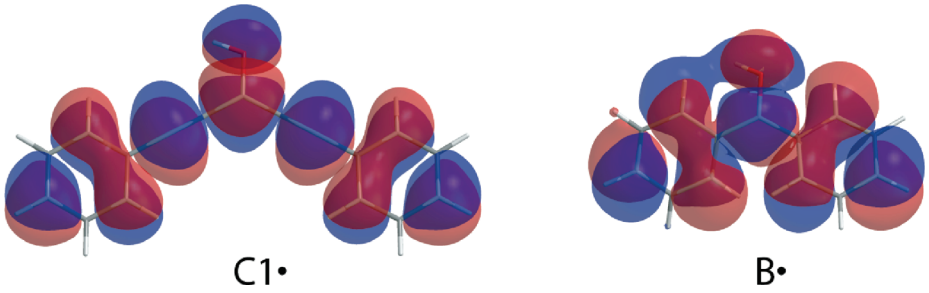

Figure 2. SOMOs of C1• and B• calculated with B3LYP/TZVP.

Chart 2

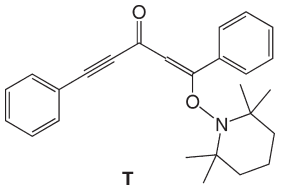

T

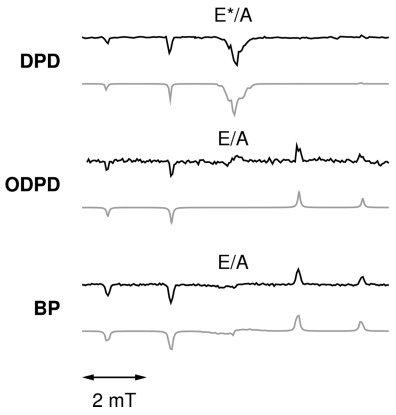

Figure 3. Experimental (black lines, integrated signal for $0.5 < t < 2$ μs) TR-EPR spectra of photoinitiators DPD, ODPD, and BP in propan-2-ol and corresponding simulations (gray lines) of the polarization pattern of the propan-2-ol-2-yl radical using either a mixture of the TM and the RPM (for DPD) or only the RPM (for ODPD and BP). The hyperfine coupling constants for the simulation of C1• and B• were taken from Table 1.

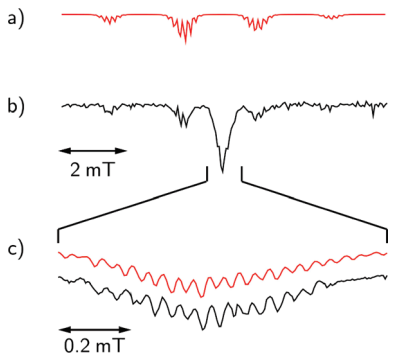

Figure 4. Experimental (b, black) TR-EPR spectrum (integrated signal for $0.5 < t < 2$ μs) of DPD and BAC in propan-2-ol and the corresponding simulation (a, red) of the polarization pattern of radical BIP• (cf. Scheme 2) using a mixture of the TM and the RPM. The signal assigned to C1• is shown with a higher resolution in (c).

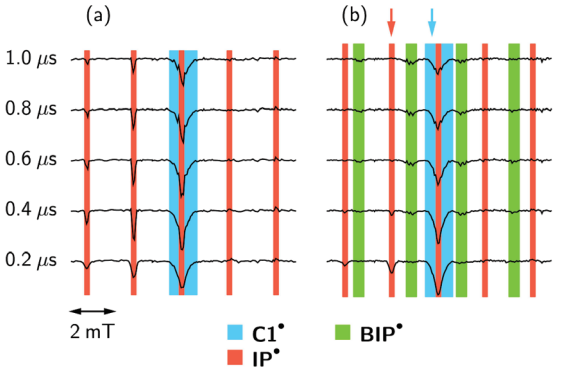

Figure 5. Slices of the TR-EPR spectra of DPD in (a) the presence of propan-2-ol and (b) upon addition of BAC. The delay times are given in the figure. The arrows indicate the field positions at which the time traces of Figure 6 were recorded.

protons, an essentially planar geometry marks the energy minimum of C1•. The slightly smaller ^{1}H hfc values for C1• show that also the connecting acetylenic bridge carries spin population. This is illustrated by the SOMOs of C1• and B• (Figure 2) and the observation that photolysis of DPD in propan-2-ol in the presence of the nitroxide TEMPO (2,2,6,6-tetramethylpyperidinoxyl) leads to the addition product T.[5]

One observation, however, is essential: whereas the line patterns of the CW TR-EPR spectra obtained upon photolysis of DPD, ODPD, and BP are very similar, significant differences exist for the relative line intensities (polarization patterns, cf. Figure 3): In the case of ODPD and BP, the low field lines appear in emission (E), while the high field lines are absorptive (A). This E/A pattern is attributed to the radical pair mechanism (RPM) of chemically induced dynamic electron spin polarization (CIDEP)[21,22] and is typical for radicals produced from the spin-relaxed triplet state. The CW TR-EPR spectrum of DPD, on the other hand, shows a significant emissive contribution (E*/A pattern) caused by the triplet mechanism (TM) of CIDEP.[23−25] The amount of admixing of the triplet- to the radical pair-mechanism depends on the rate of quenching of the triplet state with respect to its spin−lattice relaxation time, $^3T_1$.[21] This points to a higher reactivity of DPD compared to ODPD (and BP). Accordingly, the improved performance of DPD compared to ODPD found in refs 2 and 3 could tentatively be ascribed to a faster hydrogen abstraction reaction of DPD. This comparison, however, is provisional and only valid in the case of molecules of similar size (can roughly be anticipated here), and thus similar molecular rotation, which is one of the dominant factors for $^3T_1$.

3.3. Reaction of DPD with Butyl Acrylate (BAC) in Propan-2-ol. To distinguish whether exclusively the propan-2-ol-2-yl radical (IP•, Scheme 2)[5] is the radical inducing chain growth in formulations containing acrylates and propan-2-ol or whether, on a short time scale, also the radicals of the C• type react with double bonds, we have performed this

Scheme 2. Reaction Pathways for C1• and IP• in the Presence of BAC[a]

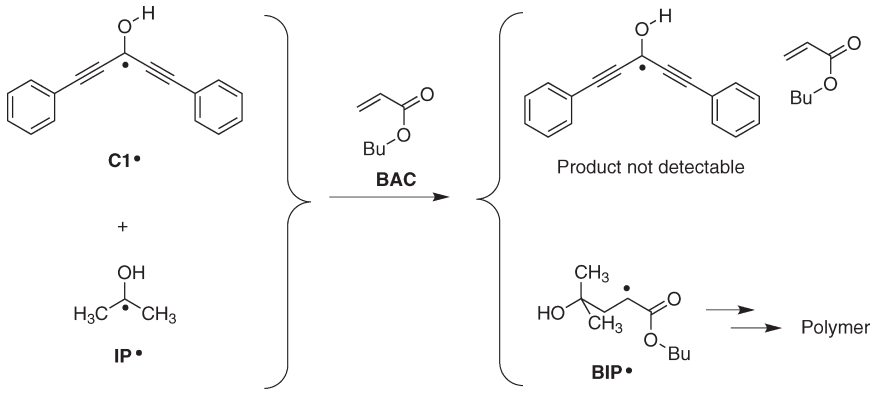

[a] The addition of IP• to the BAC double bond was found to be more efficient than the corresponding reaction of the photoinitiator radical C1•.

reaction inside the TR-EPR spectrometer using a one-way flow-system and BAC as monomer.

The TR-EPR spectrum obtained after irradiating a mixture of DPD and BAC (10-fold excess) in propan-2-ol is displayed in Figure 4b. The two main components of the spectrum are indicated in Figure 4a,c. The dominating quartet-like pattern in Figure 4a is caused by radical BIP• (Scheme 2) in which the α hydrogen atom possesses an almost identical hfc as the two equivalent β hydrogens (2.01 and 2.2 mT, respectively, 0.15 mT for the six δ Hs),[9] the remaining splittings stemming from more distant hydrogens. The second central component can be further resolved (Figure 4c) and is identical to that shown in Figure 1 representing the delocalized π radical C1• generated from DPD and IP (discussed in the previous paragraph). Notably, the signal of C1• shows identical splittings and decay times as in the absence of BAC.

This behavior becomes even more evident from Figure 5 depicting the TR-EPR spectrum of DPD in propan-2-ol in the absence and presence of BAC at various time delays after the laser pulse. Apparently the lines, which are attributed to the IP• disappear in the presence of BAC and give rise to additional lines, which can be assigned to radical BIP• (Scheme 2). The simulation (cf. Figure 4a) of the CW TR-EPR spectrum of this adduct with hfcs being essentially identical to the published values[9] renders this assignment plausible.

The attenuated reactivity of C1• is further corroborated by the time traces of C1• and IP• shown in Figure 6. While the decay of the signal attributed to IP• is dramatically enhanced in the presence of BAC, the time dependence of that of C1• is almost identical in the absence and presence of BAC. This cannot be traced back to steric hindrance (as in the case of BP) since the radical center •CR_2OH is not shielded by two directly attached phenyl groups. It is more likely that owing to the substantial delocalization of the unpaired electron within the entire π system the π character at •CR_2OH is even higher than in the BP-derived radical and the electron delocalization is even more extended leaving even less spin population at this C atom, reflected by the calculated p_z-spin population of 0.47 for the central C atom in the diphenylhydroxymethyl radical B• vs 0.38 in C1•. This behavior underpins the electron distribution predicted by the DFT calculations (Figure 2).

3.3. ^{1}H CIDNP Investigations. In-situ photolysis of DPD and ODPD in d_3-MeCN does not yield any well-distinguishable polarizations in the ^{1}H NMR spectra. With the addition of BAC, again, no polarizations upon use of the laser are observed; however, when the Hg/Xe lamp is used, weak

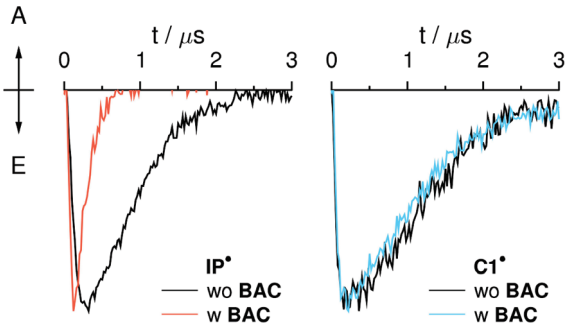

Figure 6. Time traces of IP• (left, recorded at the field position of the red arrow in Figure 5b) and C1• (right, recorded at the field position of the blue arrow in Figure 5b) in the absence (black) and presence (colored) of BAC monomer.

polarizations of the signals stemming from the acrylate are detected. In the presence of propan-2-ol, weak polarizations are detectable in the ^{1}H CIDNP experiments for the aromatic protons of the initiator (see Supporting Information) and the propan-2-ol resonances. This points at a (reversible) hydrogen abstraction of the excited triplet state of DPD (ODPD) from propan-2-ol and the formation of radicals of type C• and IP• (Scheme 2), confirming the reaction pathway developed from the CW TR-EPR measurements.

4. Conclusions

It has been shown that, under one-photon absorption conditions, the hydrogen-abstraction reaction by the excited triplet state of the ketones BP, DPD, and ODPD from a H-donor like propan-2-ol is the dominating reaction pathway for the initiation of a polymerization. The so-generated propan-2-ol-2-yl radical is able to add to the double bond of e.g. acrylates and induce chain growth (see Scheme 2). Nevertheless, there are distinct differences between BP/ODPD on the one hand and DPD on the other: the distinct polarization patterns clearly discriminate between the different one-photon reactivities observed for these initiators. While BP/ODPD exclusively display a radical-pair mechanism, a substantial admixture of the triplet mechanism is observed for DPD. This points at a more rapid and more efficient H-abstraction of DPD compared to the two remaining ketones. This finding is actually in line with product-yield-detected ESR studies from Podyakov et al. that showed a much faster H-abstraction from SDS micelles for DPD than for BP.[26]

We have observed that the acetonitrile solutions containing DPD and ODPD become strongly colored (orange-brownish) when irradiated more extensively without, however, obtaining

TR-EPR spectra or ^{1}H CIDNP signals. This may point to additional reaction pathways involving charge-separated states and polar reactions not detectable by our techniques, in line with previous product analyses.[5]

Here, we only can speculate about the reasons of the activity of DPD as a two-photon initiator. Compared to BP, DPD can adopt planar conformations because the steric hindrance of the *ortho* protons in BP does not exist in the case of DPD. This is just one of several factors enhancing the TPA efficiency[27] (among others, e.g., symmetry, dipole moment, widths of the one-photon absorption lines). One additional factor may be a differing (photo)-reactivity of distinct molecular conformations, which are selected by the two-photon process since, within the two-photon excitation, a thermal equilibration/relaxation of nonminimum energies is not possible.[28,29] It is therefore worth investigating why DPD and its derivatives display substantial TPA activity.

Acknowledgment. Funding from the Austrian FWF (P18623) and the Ciba Jubiläumsstiftung is gratefully acknowledged. G.G. and A.R. thank Dr. Toerring (Berlin) for valuable help with the TR-EPR setup and for the numerous hours spent updating and adapting the software. The authors thank Prof. M. Forbes (Univ. of North Carolina) for kindly providing an easy to use computer program for the TR-EPR simulations.

Supporting Information Available: Calculated dependence of the OH proton hfcs on the torsion angle in radicals $B^{\bullet}$ and $C1^{\bullet}$, geometries, ^{1}H CIDNP for ODPD and propan-2-ol. This material is available free of charge via the Internet at http://pubs.acs.org.

References and Notes

(1) Liska, R.; Seidl, B. *J. Polym. Sci., Part A: Polym. Chem.* **2005**, *43*, 101–111.
(2) Pucher, N.; Rosspeintner, A.; Satzinger, V.; Schmidt, V.; Gescheidt, G.; Stampfl, J.; Liska, R. *Macromolecules* **2009**, *42*, 6519–6528.
(3) Heller, C.; Pucher, N.; Seidl, B.; Kalinyaprak-Icten, K.; Ullrich, G.; Kuna, L.; Satzinger, V.; Schmidt, V.; Lichtenegger, H. C.; Stampfl, J.; Liska, R. *J. Polym. Sci., Part A: Polym. Chem.* **2007**, *45*, 3280–3291.
(4) Jockusch, S.; Landis, M. S.; Freiermuth, B.; Turro, N. J. *Macromolecules* **2001**, *34*, 1619–1626.
(5) Seidl, B.; Liska, R. *Macromol. Chem. Phys.* **2007**, *208*, 44–54.
(6) Akiyama, K.; Sekiguchi, S.; Tero-Kubota, S. *J. Phys. Chem.* **1996**, *100*, 180–183.
(7) Woodward, J. R.; Lin, T.-S.; Sakaguchi, Y.; Hayashi, H. *Mol. Phys.* **2002**, *100*, 1235–1244.
(8) Meng, Q.-X.; Sakaguchi, Y.; Hayashi, H. *Mol. Phys.* **1997**, *90*, 15–23.
(9) Weber, M.; Turro, N. J.; Beckert, D. *Phys. Chem. Chem. Phys.* **2002**, *4*, 168–172.
(10) Bargon, J.; Fischer, H.; Johnson, U. *Z. Naturforsch., A* **1967**, *22*, 1551–1555.
(11) Fischer, H.; Bargon, J. *Acc. Chem. Res.* **1969**, *2*, 110–114.
(12) Ward, H.; Lawler, R. *J. Am. Chem. Soc.* **1967**, *89*, 5518–5519.
(13) http://users.physik.fu-berlin.de/~toerring/.
(14) Frisch, M. J.; et al. *Gaussian 03, Revision E.01*; Gaussian, Inc.: Wallingford, CT, 2004.
(15) Becke, A. D. *J. Chem. Phys.* **1993**, *98*, 5648–52.
(16) Stephens, P. J.; Devlin, F. J.; Chabalowski, C. F.; Frisch, M. J. *J. Phys. Chem.* **1994**, *98*, 11623–11627.
(17) Schaefer, A.; Huber, C.; Ahlrichs, R. *J. Chem. Phys.* **1994**, *100*, 5829–35.
(18) Naguib, Y. M. A.; Steel, C.; Cohen, S. G.; Young, M. A. *J. Phys. Chem.* **1987**, *91*, 3033–3036.
(19) Livingston, R.; Zeldes, H. *J. Am. Chem. Soc.* **1966**, *88*, 4333–4336.
(20) Wilson, R. *J. Chem. Soc. B* **1968**, 84–90.
(21) Adrian, F. J. *J. Chem. Phys.* **1971**, *54*, 3918–3923.
(22) Pedersen, J. B.; Freed, J. H. *J. Chem. Phys.* **1973**, *58*, 2746–2762.
(23) Atkins, P. W.; Buchanan, I. C.; Gurd, R. C.; McLauchlan, K. A.; Simpson, A. F. *J. Chem. Soc. D* **1970**, 513–514.
(24) Wong, S. K.; Hutchinson, D. A.; Wan, J. K. S. *J. Chem. Phys.* **1973**, *58*, 985–989.
(25) Wan, J. K. S.; Elliot, A. J. *Acc. Chem. Res.* **1977**, *10*, 161–166.
(26) Polyakov, N. E.; Okazaki, M.; Toriyama, K.; Leshina, T. V.; Fujiwara, Y.; Tanimoto, Y. *J. Phys. Chem.* **1994**, *98*, 10563–10567.
(27) Pawlicki, M.; Collins, H. A.; Denning, R. G.; Anderson, H. L. *Angew. Chem., Int. Ed.* **2009**, *48*, 3244–3266.
(28) Brede, O.; Leichtner, T.; Kapoor, S.; Naumov, S.; Hermann, R. *Chem. Phys. Lett.* **2002**, *366*, 377–382.
(29) Spichty, M.; Turro, N. J.; Rist, G.; Birbaum, J.-L.; Dietliker, K.; Wolf, J.-P.; Gescheidt, G. *J. Photochem. Photobiol. A* **2001**, *142*, 209–213.